Current Progress in Gamma Ray Astrophysics (100 MeV to 10 TeV)

David A. Smith

1 Introduction

The launch of the Compton Gamma Ray Observatory (CGRO) on the Space Shuttle in 1991 coincided with breakthroughs at ground-based gamma ray telescopes, sparking renewed interest in astrophysical gamma rays from 100 MeV to 10 TeV. This talk begins with a few of the striking results from the Egret instrument on the CGRO and from the ground based gamma ray telescopes, which include observations of pulsars and Active Galactic Nuclei (AGN's). After a brief description of AGN's, the ground-based results will be interpreted in terms of gamma ray absorption by intergalactic photons through e^+e^- pair production.

The conclusion is that measuring the shape of the gamma ray energy spectra in the window between the upper reach of the satellites (about 10 GeV) and the lower threshold of the ground-based detectors (currently about 400 GeV) probes many topics of fundamental astrophysical interest: the shape of the spectrum in that window tests AGN models and acceleration mechanisms, which are related to questions about the orgin of the cosmic radiation around the 'ankle' at 10^{18} eV. The spectra for many sources of different redshifts z gives a measurement, for fixed value of the cosmological constant Ω_0, of $n(\epsilon)/H_0$, where $n(\epsilon)$ is the number density for diffuse extragalactic photons of energy ϵ (near infrared to the near ultraviolet), and H_0 is the Hubble constant. The soft photon density $n(\epsilon)$ in turn probes details of galactic evolution in the early universe and mixed cold and hot dark matter models.

The rest of the talk discusses how to open the window $20 < E_\gamma < 200$ GeV. First I review current gamma ray telescopes, and then describe the next generation of detectors now coming online. Finally I outline how to use existing solar power plants as gamma ray detectors.

2 Recent Results from Gamma Ray Telescopes

2.1 Satellite-based Gamma Ray Telescopes

Figure 1 shows the Compton Gamma Ray Observatory, which is roughly the size of a Volkswagen Beetle (Kanbach et al, 1988; Fichtel 1993; See also Weekes 1988, page 90). There are four detectors on board: Osse, the Oriented Scintillation Spectrometer Experiment, studies low energy gamma rays. Comptel, for Compton Telescope, images soft gamma rays up to the Egret energy range (see figure 13). Batse, the Burst and Transient Source Experiment, studies the gamma ray bursters, a fascinating topic that is unfortunately beyond the scope of this talk. Egret, the Energetic Gamma Ray Telescope (the lower dome in figure 1), measures the direction of high energy gamma rays (10 MeV to 30 GeV) to 5 arc-minutes by tracing the electron and positron from pair production

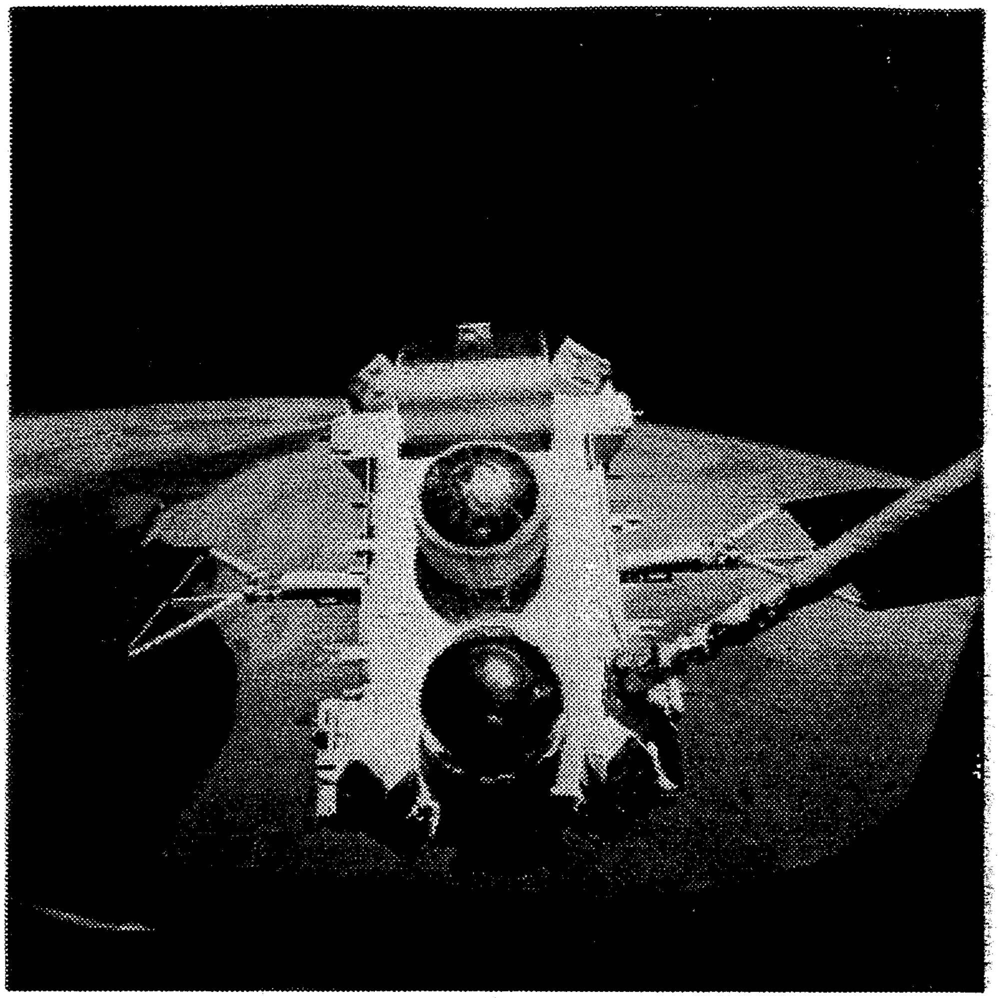

Figure 1: The Compton Gamma Ray Observatory.

in spark chambers. A large sodium iodide crystal mounted behind the spark chamber gives the energy, all of which is encased in scintillator to reject charged particle backgrounds. Perhaps the most striking result from the Egret instrument is that while the diffuse distribution for $E_\gamma > 100$ Mev is dominated by the plane of the milky way galaxy, most of the discrete sources are extremely distant. Figure 2 shows the sky as seen in this energy range. Over 40 AGN's, mostly BL-Lac objects and "blazars" have been detected (Fichtel 1994, Stiavelli 1994). In addition, there is a comparable list of marginal detections, and a comparable list of unidentified sources at high galactic latitude.

Figure 13 shows the gamma ray spectrum from the Crab nebula over the energy range from Comptel to Themistocle (more on Themis later). A two-component model for the Crab nebula, dominated by synchrotron emission up to 100 MeV and then by inverse Compton scattering through 10 TeV, fits the data. The long lever arm that comes from combining the ground-based and satellite measurements is a powerful tool for discriminating between different models (Harding 1994).

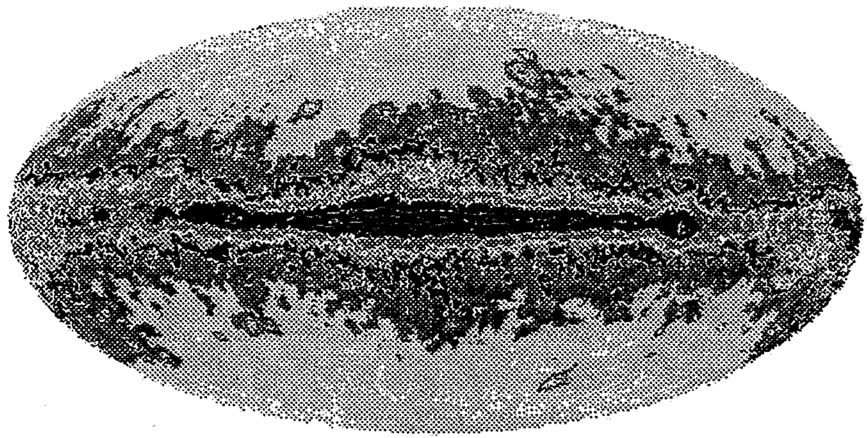

Figure 2: Map of the gamma-ray sky, $E_\gamma > 100$ MeV, measured by Egret. The dark band is the diffuse radiation along the plane of the milky way.

2.2 Ground-based Gamma Ray Telescopes

As shown in figure 13, the Crab nebula has been observed by a number of Čerenkov telescopes. The first was the Whipple telescope at Mt. Hopkins, Arizona, using the imaging technique (Vacanti 1991). The Whipple telescope is shown in figure 3. The Themistocle (Baillon 1992) and Asgat (Goret 1993) experiments pioneered the time sampling method at Themis in the French Pyrenees. Since then, other groups have also seen the Crab, mainly using the imaging method (Krennirich 1993). Only one other galactic source has been detected by a ground-based gamma-ray telescope: the pulsar 1706-44, visible in the Southern hemisphere (Ogio 1993).

The list of reproducible ground-based observations is completed with only one more entry: the blazar Markarian 421 (Punch 1992). Mrk 421 is both the dimmest and the closest extragalactic source in the Egret catalog (redshift $z = 0.031$). The casual observer might think that the field is quite poor, with only three detectable sources. But the detection of Mrk 421 when so many brighter sources are invisible is quite remarkable. For example, the blazar 3C279 ($z = 0.54$) has been seen by Egret to flare to 30 times the luminosity of Mrk 421 and stands out in figure 2 (Kniffen 1992). Why isn't 3C279 seen, while Mrk 421 is? The most reasonable explanation is that TeV gamma-rays above some energy are absorbed while crossing space through the mechanism

$$\gamma\gamma \rightarrow e^+e^-.$$

This process will be discussed below. An alternate explanation, that the acceleration mechanism in AGN's (except for Mrk421!) 'runs out of gas' between satellite and ground energies (like the roll-over in the Crab spectrum in figure 13) would be tested by measuring the energy roll-over for many sources at different redshifts.

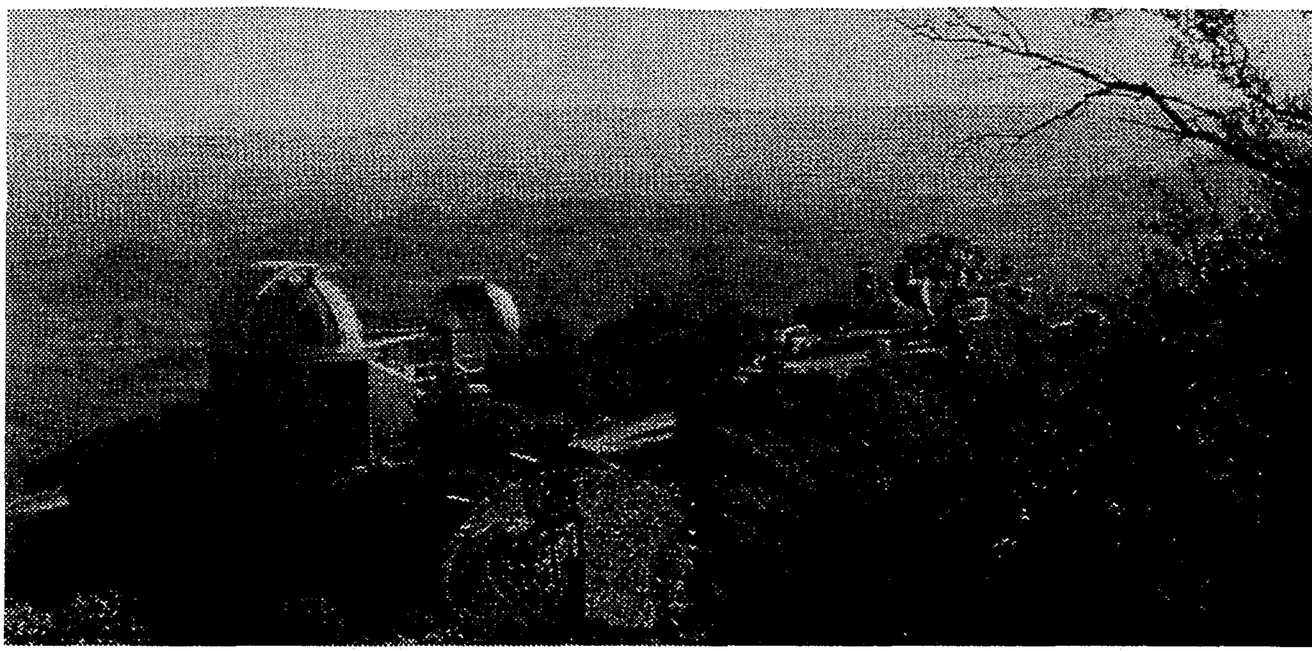

Figure 3: The Fred L. Whipple Observatory on Mt. Hopkins in Arizona. The 10 meter Čerenkov telescope is visible at the right. A second 10 meter imaging telescope is now being commissioned, 100 meters away, and should give both finer angular resolution and a lower energy threshold.

2.3 Active Galactic Nuclei

Quasars (also QSO's, or Quasi-Stellar Objects) were discovered in 1963 with radio telescopes. Since then, they have been studied at all wavelengths and with increasing resolution. They are both the most distant objects known and are some of the brightest sources in the sky. To be so bright yet so far means that they are amazingly powerful.

What are they? The biggest telescopes can see about one million faint blue galaxies in any square degree of the sky. About one in 5000 of these galaxies has an active nucleus, that is, a bright point source at the center of the galaxy is distinct from the dimmer, more diffuse body of the galaxy. These AGN's are categorized according to their emission at different wavelengths: some category names are OVV (Optically Violent Variable), "radio bright", "flat radio", "Seyfert I and II", "BL Lac", and "blazar". Quasars then are just one part of this zoo (see Stiavelli 1994).

Acceleration models try to extend the successful theories explaining the pulsar spectra. A pulsar is a spinning neutron star left over after a supernova. The pulsar is surrounded by matter falling into the neutron star, either from a diffuse nebula, from an accretion disk, or from a companion star. The charged particles in the magnetic field of the pulsar emit synchrotron light, as in figure 13. At higher energies, the scattering of electrons in the disk generates gammas by the inverse compton process. Various models are summarized in table 1.

Pulsar-type models cannot explain the immense power output of the AGN's. A unified model has emerged that explains the continuum of active galaxy types and does a better job of reaching the needed power range. An AGN would be a supermassive black hole (over 10^9 solar masses) surrounded by a disk of matter falling into the black hole. The tremendous energy released in this process shoots out as a narrow particle jet perpendicular to the disk. The source of the power is the gravitational potential energy of the matter in the field of the black hole, and about 70% of the rest mass is converted into kinetic energy. The broad range of different types of AGN's can be understood simply as different angles of the jet relative to an earthbound observer (see figure 4). In Mrk 421 and 3C279 we happen to be looking straight down the jet, and the power output is roughly constant from radio to gamma. In a Seyfert I type galaxy, we are looking edge-on at the disk, and most of the radiation is absorbed. These jets may be the orgin of the highest energy cosmic rays. But only the gamma rays can be observed directly (since magnetic fields confuse the charged particle directions), and only the ground-based detectors have the flux sensitivity at needed higher energies. The detailed mechanisms are again thought to be some combination of those in table 1.

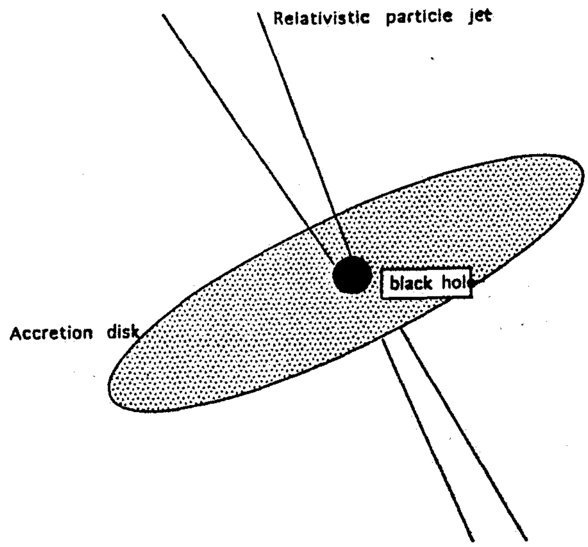

Figure 4: Artist's conception of an Active Galactic Nucleus (AGN).

POWER SOURCE	ACCELERATION MECHANISM			
	Dynamo $E_p^{max} \le e\frac{v\times B}{c}R$	Shock $E_p^{max} \simeq e\frac{u_1}{c}BR_s$	Reconnection $E_p^{max} < e\frac{v}{c}BR$	Plasma Turbulence $E_p^{max} \simeq eBR$
Pulsar Rotation $L < 10^{43}$ **erg/s**	$< 10^{14}$ eV	$< 10^{18}$ eV		
Accretion $L_{NS} < 10^{38}$ **erg/s**	$< 10^{17}$ eV	$< 10^{16}$ eV	$< 10^{14}$ eV	$< 10^{16}$ eV

Table 1: Acceleration models for gamma-ray sources (from Harding 1994).

3 Gamma Ray Absorption by Starlight

A gamma-ray of energy $E_0(1+z)$ from an AGN at a redshift z travelling to earth traverses a column of 'soft' photons of energy ϵ and density $n(\epsilon)$. The probability for the gamma to survive the trip is $e^{-\tau}$, where the 'optical depth' τ is, schematically, $\tau \propto \sigma r n(\epsilon)$, where the distance r is cz/H_0. The relevant cross-section σ is for pair production, $\gamma\gamma \rightarrow e^+e^-$, given by

$$\sigma\Big(E_\gamma(z), \epsilon(z)\Big) = \sigma_0(1-\beta^2)\Big[2\beta(\beta^2-2) + (3-\beta^4)\ln\Big(\frac{1+\beta}{1-\beta}\Big)\Big]$$

with $(1-\beta^2) = \frac{2m_e^2}{E_0\epsilon_0 x(1+z)^2}$ and $\sigma_0 = 0.125$ barns [1]. Here, $x = (1-\cos\theta)$ is the angle between the two photons, E_0 and ϵ_0 are the energies in the rest frame of the observers, and $E(z), \epsilon(z)$ are the redshifted photon energies.

The general expression for the optical depth is then

$$\tau(E_0) = \frac{c}{H_0}\int_0^z dz' \frac{(1+z')}{(1+\Omega_0 z')^{1/2}} \int_0^2 dx \frac{x}{2} \int_{\epsilon_1}^\infty d\epsilon_0 n\Big(\epsilon_0(1+z')\Big)\sigma\Big(2x\epsilon_0 E_0(1+z')^2\Big)$$

where ϵ_1 is the threshold energy,

$$\epsilon_1 = \frac{2m_e^2}{E_0 x(1+z')^2}$$

and $\epsilon_0 = \epsilon/(1+z')$. For a 1 TeV gamma, absorbing photons around the near infrared (2 μM $\simeq 0.6$ eV) dominate. (In fact, because of the $(1+z)^{-2}$ term, the near infrared to near UV photons dominate for all gamma ray energies).

The crux of the matter is the target photon density, $n(\epsilon)$. Figure 5 summarizes knowledge of the diffuse extragalactic photon spectrum for all wavelengths as of a few years ago. No reliable measurements have been made around 2 μM, only upper limits. Subtraction of local IR sources, *e.g.* planets and dust, complicates the measurement. Detailed models of the shape of the IR spectrum are sums of different components, so that a power law is a rather poor model.

Nevertheless, the extragalactic IR spectrum is rich with information. The theory of early galactic evolution is closely tied in with mixed cold and dark matter models and predict different IR densities (MacMinn 1994). So it is worth the excercise to choose a spectrum shape, such as a power law,

$$n(\epsilon) = k\epsilon^{-\gamma}$$

and to calculate the amount of absorption. In that case, and choosing $\Omega_0 = 1$ for the cosmological constant, the expression for τ simplifies to

$$\tau(E_0, z, \gamma) = 2\sigma_0 \frac{c}{H_0}\frac{k}{\gamma+1}\Big(\frac{E_0}{m_e^2}\Big)^{\gamma-1}\frac{(1+z)^{2\gamma-\frac{1}{2}}-1}{2\gamma-\frac{1}{2}}\int_0^1 d\beta \quad \beta(1-\beta^2)^{\gamma-2}\sigma(\beta).$$

The numerical solution for the integral over β for different γ is shown in figure 6a. Figure 6b shows

[1] 1 barn $= 10^{-24}$ cm^2.

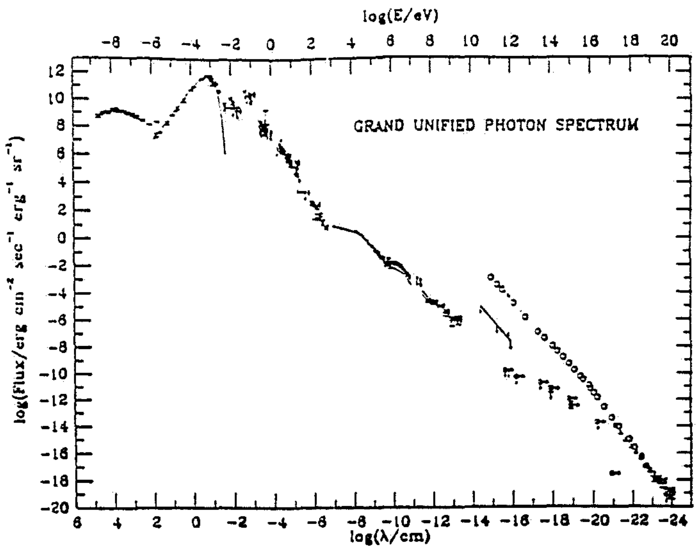

Figure 5: Extragalactic differential photon flux. No measurements exist for high energy gamma rays so the charged particle fluxes are used as upper limits (open circles) (Ressel & Turner 1989).

the optical depth as a function of redshift for some different values of E_0, using

$$n(\epsilon) = 0.001 \cdot \epsilon^{-2.55}$$

following Salamon, Stecker, and DeJager (1994), which is consistent with figure 5. At 1 TeV and $z = 0.031$, Mrk 421 suffers almost no attenuation. 3C279 on the other hand should be invisible ($z = 0.54$). Extending the energy sensitivity into the gap between ground devices and satellites will permit measurement of the roll-off zone, and hence will constrain $n(\epsilon)/H_0$ and, to a lesser extent, Ω_0.

4 Gamma Ray Detection

Up to this point I've only discussed the results from the various gamma ray detectors. I now turn to how the instruments work, and how to open the energy window.

4.1 Satellites

The high energy reach of a satellite detector is limited by the relatively small mass and volume that can be sent aloft. The collection area of Egret varies with energy but is about 1500 cm^2. For an observation period of 10 days on a typical source, that gives only a few photons in the highest energy bins. Good energy resolution at high energy requires a deep detector: depth times area means mass.

On the other hand, satellite-based instruments have many advantages compared to ground-based telescopes using the atmospheric Čerenkov method. Foremost is the very low background, and the broad angular aperture. Large angular acceptance means not only that large (30° squared) pieces of

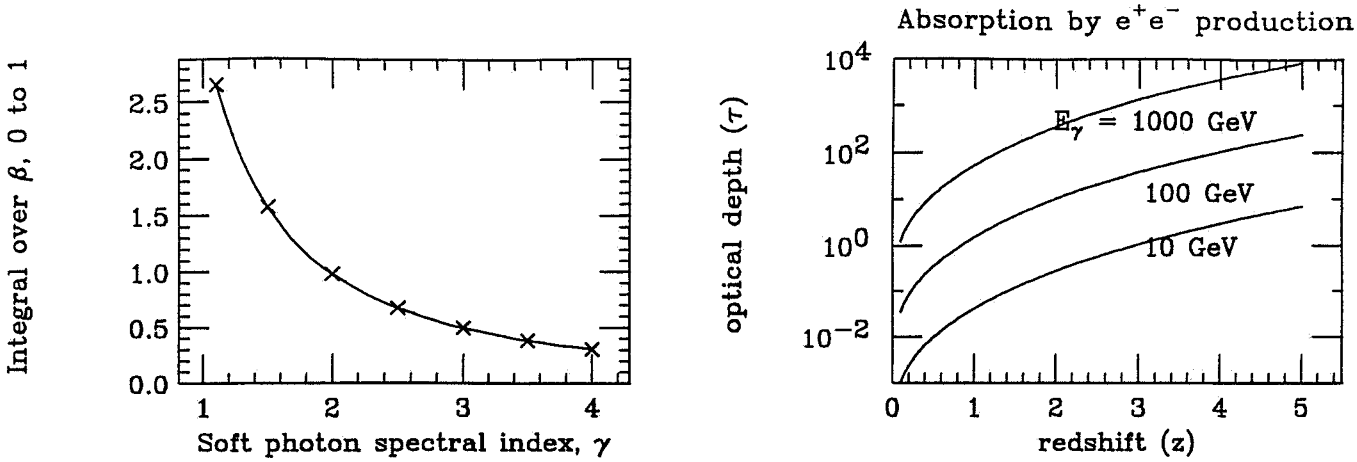

Figure 6: a) Numerical value of the pair-production cross section times photon density integral. b) Optical depth τ as a function of redshift z for some different gamma ray energies.

the sky can be viewed at once, which permits searches for unexpected sources, but also means that diffuse or extended sources can be studied. Ground-based techniques are sensitive only to point sources.

Two successors to Egret are being studied. Agate is an extension of the Egret design: a much larger spark chamber, useful up to 50 GeV or so (Hunter 1993). Glast is a completely new device, based on silicon strips (Godfrey 1993). It would reach up to 300 GeV. However, the only satellite project that has been funded is Integral, which runs up to about 2 MeV. It seems unlikely that either Agate or Glast would fly before 2010. This is one reason that NASA is urged to prolong the CGRO mission as long as possible, and why ground-based experiments look good now.

4.2 Ground-based Detectors

Figure 7 gives a nice overview of cosmic ray detection methods. Up to 10 GeV, balloons and satellites are best. (An important technical development in the last few years has been the use of long-duration balloon flights over the south pole). Beyond that, the only way to have a large collection area is to allow the primary particle to shower in the atmosphere, and to reconstruct the energy, direction, and species of the primary particle by sampling some part of the cascade of secondary particles. Above 10^{17} eV, nitrogen fluorescence allows the "Fly's Eye" technique, with enormous sensitive areas and full longitudinal reconstruction of the shower that allows composition studies. Above about 20 TeV, enough charged particles reach the ground to enable use of scintillator arrays. No scintillator array has observed a discrete gamma-ray source, probably because the background rejection is poor (because the angular resolution is spoiled by multiple scattering in the shower tail), or because the spectra have petered out (thought to be the case for pulsars, see fig 13), or due to increased absorption at higher energies. (The energy threshold for a charged particle array depends on the altitude and the density of the array: the Tibet array, above 4000 m, is sensitive below 10 TeV.)

At 1 TeV and lower, the only part of the shower that reaches the ground is the Čerenkov light

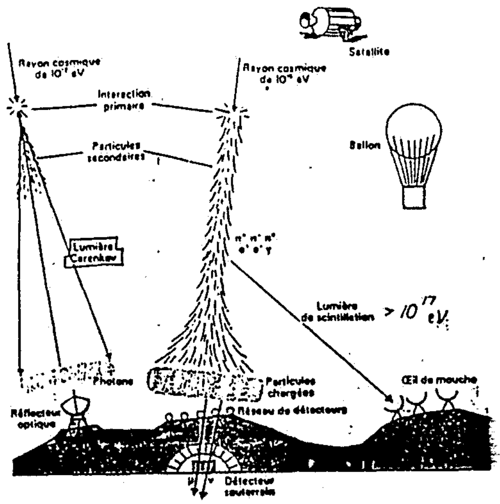

Figure 7: Cosmic ray detection methods. Gamma rays from 20 GeV to 20 TeV can be measured using the atmospheric Čerenkov technique (ACT).

generated by ultra-relativistic charged secondaries near shower maximum. To remind the reader, Čerenkov light is the radiation generated by a charge moving faster than the speed of light in the medium, $\beta c > c/n$ (22 MeV for an electron in air at sea level, 4.6 GeV for a muon). The light is generated at an angle $\cos\theta_C = 1/n\beta$, and the number of photons with wavelength $\lambda_1 < \lambda < \lambda_2$ emitted per unit length is

$$\frac{dN}{dx} = 2\pi\alpha\Big(1 - \frac{1}{\beta^2 n(\lambda)^2}\Big)\Big(\frac{1}{\lambda_1} - \frac{1}{\lambda_2}\Big).$$

For a 50 MeV electron (or a 10 GeV muon) in air, this gives $dN/dx \simeq 40$ photons per meter and $\theta_C = 20$ mR, decreasing with altitude.

The observations of the Crab, PSR 1706-44, and Mrk 421 have proved the power of the Atmospheric Čerenkov Technique (ACT). It took over twenty years to achieve these results, basically due to two difficult-to-manage backgrounds. The first is the night sky light. A Čerenkov telescope minimizes this background using fast photomultipliers and a narrow angular aperture (see table 2). Even so, the telescopes can only run on dark, clear nights, which limits observation time. (Charged particle arrays run all the time).

The other background is from cosmic rays: the charged particle flux is typically 1000 times more than the gamma source (depending on the telescope design and the source). The art in the ACT is to reject the background while maintaining high efficiency for the signal. Hadron/gamma separation is possible because of basic differences between the two types of showers. Figure 8 illustrates the point. In a pure electromagnetic shower, both the spatial and angular distributions of Čerenkov light on the ground are uniform and narrow. The light from hadron showers is more irregularly distributed. This fundamental difference is exploited with two complementary techniques, imaging and timing. The other important key to signal-to-noise reduction is good angular resolution: even a weak point source stands out against an isotropic background if the angular binning is fine enough.

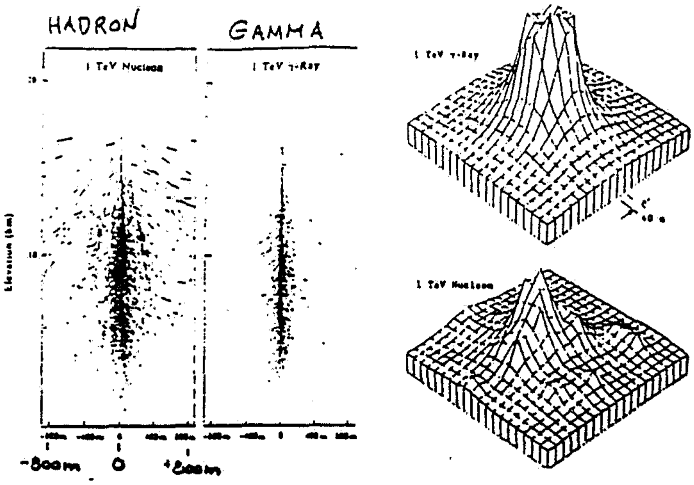

Figure 8: Simulated particle cascades. The Atmospheric Čerenkov Technique favors gamma showers by selecting narrow, uniform distributions of light.

4.2.1 Imaging: The Whipple Čerenkov Detector

Figure 3 shows the Whipple Observatory run by the Smithsonian Institute, at Mt. Hopkins in Arizona. The 10 meter Čerenkov telescope is visible at the far right. Figure 9 shows the image of an electromagnetic shower superimposed on the phototube array in the focal plane of the mirror, and some of the parameters used to characterize the image.

The particle shower begins to develop at about 20 km above sea level, and is biggest around 10 km. Since $\theta_C \simeq 10$ to 15 mR, the light pool has a radius of about 120 meters. The 70 M^2 Whipple telescope samples less than 1% of the light pool.

The core of the shower generating light is about 20 meters wide, so the angular width of the image is only a couple of millradians. On the other hand, the shower develops over several kilometers, so the longitudinal image depends on where the impact point of the shower is relative to the mirror: if the shower points down the optic axis, the image is round. If the shower is offset, then the projection of the cigar-like shower in the focal plane is up to 20 mR long. This determines the scale of both the pixel size and the mirror aperture.

The focal plane of the Whipple mirror contains an array of 108 phototubes, as shown in figure 9. The "azwidth" distribution is broader for hadron showers than for gamma showers, and selecting small azwidth gives about a factor of 100 background rejection. The "distance" variable is an estimator of the shower direction.

4.2.2 Timing: ASGAT and Themistocle

The other approach is to measure the photon arrival times at several places in the light pool. The times are fit to a conical surface, giving the shower direction. This is shown in figure 11. Furthermore, because of the irregular structure of the hadronic showers, a quality cut on the cone fit rejects background. Figure 10 shows the Themis site, where the ASGAT and Themistocle experiments both detected the Crab nebula.

NIGHT SKY NOISE CONTRIBUTION (Poisson fluctuations)	
$N \propto \sqrt{\Omega A \tau \eta \phi}$	
Ω :	Solid angle subtended by detector
A:	Area of mirror
τ :	Electronic integration time constant
η :	photon detector quantum efficiency
ϕ :	Photon flux from night sky background
ČERENKOV LIGHT SIGNAL	
$S \propto E\eta A$ (for gamma energy E, to first order)	
MINIMUM SHOWER ENERGY THRESHOLD	
$E_T \propto N/S \propto \sqrt{\frac{\Omega\tau\phi}{A\eta}}$	
FLUX SENSITIVITY	
$N_\sigma \propto \frac{A_\gamma T^{1/2} E^{0.8-\gamma}}{A_h^{1/2}\Omega^{1/2}}$	
A_γ:	Collection area for γ-rays (energy dependent)
A_h:	Collection area for hadron showers (energy dependent)
T :	Total observation time
γ:	Power law exponent for γ-ray source

Table 2: Design optimization of an atmospheric Čerenkov detector (from Fegan 1992, see also Weekes 1988).

Energy resolution is the other experimental issue. To a first approximation, the number of photons (i.e. total pulseheight in the detector) gives the energy of the primary. But there are two problems: smearing, and calibration. Smearing comes from the variation of depth in the atmosphere of the initial interaction, from fluctuations in the shower development, and from uncertainty in the center of the light pool. Calibration depends heavily on Monte Carlo simulations of the shower development and the detector response. Shower development depends both on the fragmentation in the initial collisions and the composition of the background hadrons. The detector response includes effects such as the attenuation length of the ultraviolet component of the signal, which can vary depending on atmospheric conditions. Projects are underway to refine these calibrations using single muons and fiducial stars.

4.3 2^{nd} Generation Čerenkov Detectors

Table 2 summarizes the parameters involved in designing a Čerenkov telescope. Many approaches are being implemented around the world to enhance sensitivity and to lower the energy thresholds. For example, the Whipple collaboration has built a second 10-meter telescope to improve the angular resolution with a stereo view of the shower. The Hegra experiment, at the Astrophysical Observatory

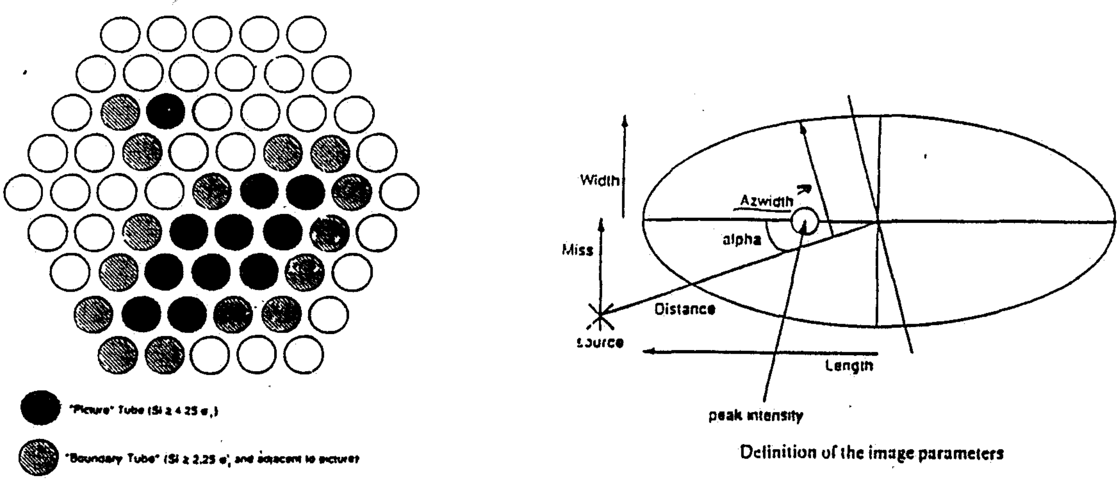

Figure 9: Illustration of a shower image in the phototube array at the focal plane of the Whipple mirror. Selecting small "azwidth" gives about a factor of 100 hadron rejection (Reynolds 1993).

in the Canary Islands, is building 5 smaller telescopes, and has an extensive array of charged particle detectors. I will go into detail only on the two projects in which I am personally involved.

4.3.1 CLUE

Referring to Table 2, reducing the night sky flux ϕ gives leeway on the other parameters. Since celestial ultraviolet light is absorbed in the ozone layer, and since the showers develop below the shower, measuring UV Č-light instead of visible light could be a good idea. This is the basic idea of Artemis (Urban 1988), which mounted solar blind phototubes on the Whipple telescope, and ran when the moon was up. Very recently they detected the Crab, after a difficult analysis that required detailed modeling of the backgrounds from single muons. The angular size of the showers is larger in the UV since one is sampling the shower tail. They will now attempt to see the displaced shadow of the moon to search for primordial antimatter.

CLUE tried the same physics, but even farther into the UV, using photosensitive wire chambers with TMAE as the photocathode. The total collection efficiency is very small since in the region where the TMAE quantum efficiency is large (below 200 nM), UV-oxygen absorption kills the signal, whereas beyond 230 nM where the Čerenkov signal is appreciable the TMAE quantum efficiency has vanished. Those photons that are collected come mainly from single muons, meaning that hadron showers are favored over gamma showers, or from electrons in the shower tail, meaning that multiple scattering is large and the intrinsic angular resolution is poor.

4.3.2 CAT

Again referring to table 2, another approach is to squeeze τ and Ω to the limits imposed by the shower shape. Then you can relax the area A. This is the philosophy of the CAT project, now under construction at the Themis site (CAT = Čerenkov Array at Themis). In fact, the sensitivity improves faster than the square root of the collection efficiency because of the narrow dispersion

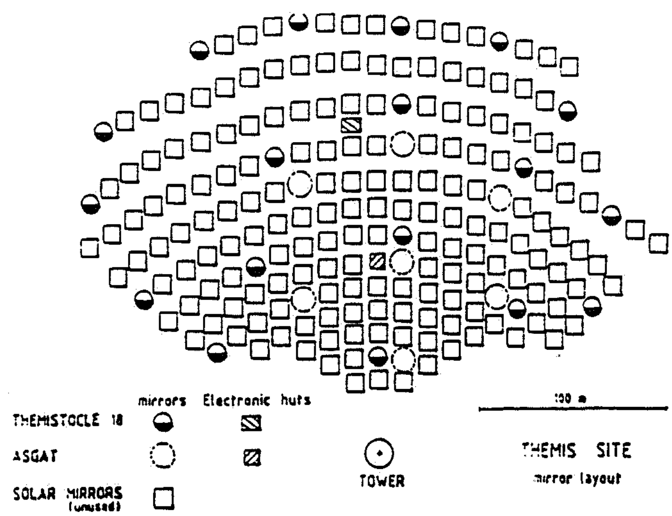

Figure 10: Themis, in the French Pyrenees, was developed to test solar electrical generation (mirrors focussed on a boiler in a central tower). Asgat and Themistocle have run successfully there, and CAT is under construction. The 8,000 m^2 of mirrors could provide an $E_\gamma > 20$ GeV gamma-ray telescope.

phototubes used, as well as the improved optics (more isochronous, smaller aberations). Energy threshold and flux sensitivity are expected to be better than for Whipple (or, about the same as Whipple with ongoing upgrades), with only 23% of the mirror area. Figure 12 shows the expected sensitivity of CAT to 3C279. The curve labeled 3C279 is a convolution of the extrapolated power law spectrum from Egret, the infrared gamma-ray absorption as calculated in figure 6b, and the detector acceptance. At Whipple's current threshold of 400 GeV, 3C279 is undetectable. At 200 GeV, it should outshine the Crab.

5 How to Get to the 10 GeV Region

At this point, I hope to have convinced the reader that gamma ray measurements in the 1 TeV region are understood, and that it is very desireable to extend sensitivity down to satellite energies. The extension to low energy should be envisaged as an extrapolation of the existing imaging techniques. Simple scaling of the instrument characteristics should be measured first in terms of the number of collected photoelectrons per shower. However, this signal S competes with the noise, B. The detector sensitivity is proportional to $S/\sqrt{B}$. As a consequence the threshold energy for gamma events varies not linearly but only as the square root of the collection performance.

This scaling law yields an unrealistically large mirror for a 10 GeV threshold if the extrapolation is based on the first generation of imaging devices. The second generation is now putting Table 2 to the test. These improvements, which all affect the angular and time resolution, are approaching the asymptotic limits imposed by the angular size of the gamma showers and by the dispersion in the time of arrival of the Čerenkov photons (unless improvements in phototube quantum efficiency are made). When the night noise is reduced to below about 0.1 photoelectrons per 10 ns then the amplitude dispersion of the PMT becomes critical. Within a year or two, when the projects now under construction have been commissioned, the ground from which to make extrapolations will be

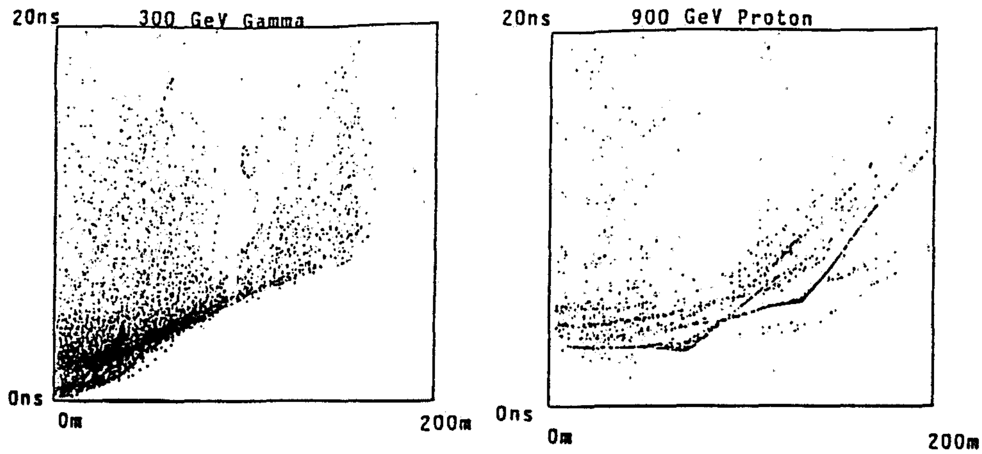

Figure 11: Principle of the wavefront sampling method of shower reconstruction: the light from an EM shower arrives like a cone, while a hadron shower is more like a superposition of many smaller cones.

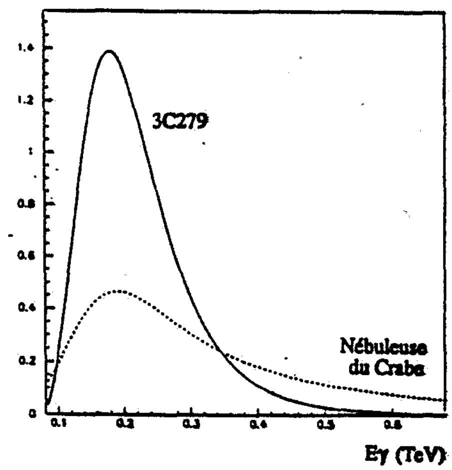

Figure 12: Expected sensitivity of CAT for the Crab nebula and for the blazar 3C279, including an estimate of infrared gamma-ray absorption.

more solid.

5.1 Electrons Replace Hadrons as the Dominant Background

The hadrons which in the present experiments constitute the bulk of the events from which the gamma signal must be sorted out (on the basis of their slender profiles) will give only little concern at 10 GeV, as their Čerenkov light yield will have faded away. Their main contribution was through secondary π^{o}'s whose energy is too low for primaries in the 10 GeV range.

On the other hand, at low energies cosmic ray electrons increase proportionately. Near 10 GeV they furnish the major part of the remaining background events. The electron showers are essentially like gamma showers, so that this background is genuinely irreducible. (The only rejection method would be to veto the event on the basis of the electric charge of the primary, which can be done only for a satellite detector). For ground-based ACT detection the electrons will remain in the final event sample after gamma selection. The electrons form a smooth, nearly isotropic angular distribution above which a gamma point source signal will stand out. The best possible angular resolution becomes the essential instrument characteristic.

Detection sensitivity when there is background contamination cannot be judged simply by the number of signal events. It must be evaluated in terms of the statistical significance of the signal, which is given again by $S/\sqrt{B}$. Here, B is the irreducible contamination by hadron and electron events. This leads to a general trend of sensitivity degradation with decreasing energy. The hadron and electron fluxes vary roughly as $E^{-2.7}$ and $E^{-3.3}$ power laws, respectively, so that the square root of the integrated flux varies roughly as $1/E$. A point source having a typical E^{-2} differential spectrum could be observed with about a constant level of significance at all energies. However, the price to pay to obtain this significance level is higher at small energies, since the decrease in Čerenkov photon yield must be compensated for by a larger collection area.

5.2 Light Pool Sampling

An alternative to the imaging method could be the light pool sampling method. The method, based on a distributed set of many independent mirrors, may be better suited for the extension to lower energies requiring a large collection area. The method relies on the hadron/(e or γ) selection on the basis of the patchy versus homogeneous distribution of Čerenkov photons in the mirror field. The hadron/gamma selection should be about as efficient as for imaging. This is supported by simulation studies. However, reconstruction of the shower axis is not trivial and cannot directly exploit the slender form of the gamma showers. At lower energies, the shower is shorter and the cone becomes a sphere. A fit to a sphere does not uniquely determine the shower direction, and hence an independent measure of the impact point of the shower is needed. This can be done by measuring the number of photons at different points in the light pool.

It is rather unlikely that the sampling method would permit as fine a measurement of the propagation direction as by imaging. Efforts are being pursued to establish the strategy, to conceive a realistic imaging device, and to evaluate its cost and performance. Two concepts have been proposed, both based on fixed mirrors and movable cameras. They differ in the choice of either a single big bowl (like Arecibo) or several close-by elements. Most of the work remains to be done.

5.3 The Solar Plants

Solar power at the industrial scale was explored in the 1980's. In the United States, France, and the Soviet Union, large mirror arrays tracking the sun were focused on boilers at the top of central receiver towers. The projects were abandoned, at least in the short term, when the price of oil dropped late in the decade.

The angular size of the sun is close to that of an air shower. Hence, while the solar arrays are not perfect for gamma ray astronomy, they aren't too far off, and they represent an investment of around a hundred million dollars. Two of these plants are under serious study for use a Čerenkov telescopes. Solar-1, near Barstow, California, is the focus of the LACE collaboration, and tests of the tracking, background light, optical quality, etc are now underway (Tumar 1991, Covault 1994). The Themis array is shown in figure 10. The two sites have different strengths, summarized in table 3. Secondary optics have to be put in place of the solar furnace, that is, at the general focus, in order to collect the photons from each heliostat independently and keep tight timing.

	Solar-1	Themis
No. Heliostats	1800	160
Heliostat area	40 m^2	50 m^2
Array diameter	540 m	250 m
Altitude	600 m	1700 m
Latitude	35^0 N	42.5^0 N
Optics	Fixed focal length	Good
Spot size	2 to 3 m	1.5 to 2.5 m
Pointing	Good (0.05^0)	Good
Light pollution	Xenon flashers, bright low haze	Village
Access	Daytime power company	Physicists only
Elevator	No	Yes
Lightening, snow	No	Some
Dust	Some	No
Infrastructure	Power co. maintains mirrors	Existing exp'ts

Table 3: Comparison between Themis and Solar-1 mirror arrays (Tumar 1991, Covault 1994, Paré 1994).

6 Conclusions

	Raw rate ($10^{-8} cm^{-2} s^{-1}$)	After cuts (Hz)
γ_o (Crab)	1	0.3
e_o (Electrons)	2.5 deg^{-2}	0.08
h_o (Hadrons)	600 deg^{-2}	0.03
$\gamma_o/(e_o + h_o)$	1/600	2.7/1

Table 4: Simulated events rates at the Themis array (Paré 1994).

Table 4 summarizes results of a simulation of a 20 GeV array using the Themis solar plant. A 7σ signal from the Crab could be acquired in about 5 minutes, and a 5σ signal for 50 mCrab source would take 10 hours. Any Egret source in the field-of-view is detectable. The Themis angular resolution is better than for Egret, and so, for example, the northern of the eight unidentified high galactic latitude sources could be scrutinized. The spectra roll-off for several sources in the Egret AGN catalog would allow the absorption-based $n(\epsilon)/H_0$ measurement, which in turn constrains mixed hot and cold dark matter models.

We are on the verge of understanding some basic mysteries of astrophysics. Ground-based gamma ray astronomy provides a big piece to the puzzle. It is limited in some ways: intergalactic absorption restricts our view of the most distant objects; Čerenkov telescopes cannot measure diffuse sources, or map large pieces of the sky; gamma rays probe only outer parts of the source. But every technique has its limits. When information from satellite-based and ground-based gamma ray telescopes will be combined with results from the projected neutrino telescopes and the very large scintillator arrays, several questions will certainly be answered.

Bibliography

- P. Baillon *et al* (1992), in Proc. 26^{th} ICHEP, Dallas (to appear in AstroParticle Physics).
- C. Covault (1994), "Report on Heliostat Tests at Solar One Site" (unpublished).
- D.J. Fegan, "The Atmospheric Čerenkov Technique: Overview of 2nd Generation Detection Systems", in "Towards a Major Atmospheric Čerenkov Detector", Palaiseau, 1992.
- C.E. Fichtel *et al* (1993), "The Compton Gamma Ray Observatory", Scientific American, December 1993.
- C.E. Fichtel *et al* (1994), "The First Energetic Gamma-ray Experiment Telescope (EGRET) Souce Catalog" (preprint).
- G.L. Godfrey, "Gamma Large Area Silicon Telescope (GLAST)", in "Towards a Major Atmospheric Čerenkov Detector - II",Calgary, 1993.
- P. Goret *et al*, "Observations of TeV Gamma Rays from the Crab Nebula", Astr. Astrophys. **270** (1993) 401.
- A.K. Harding, NASA/GSFC (1994), in Proc. Snowmass workshop on Astroparticle Physics in the Next Millenium.
- S.D. Hunter *et al*, "The Advanced Gamma-Ray Astronomy Telescope Experiment (AGATE): New Satellite Instrumentation Beyond EGRET", in "Towards a Major Atmospheric Čerenkov Detector - II",Calgary, 1993.
- G. Kanbach *et al*,.1988, Space Science Reviews, **46**, 69.
- D.A. Kniffen *et al*, (1992) Ap. J. **411**, 133.
- F. Krennerich *et al* (1993), in Proc. 23^{rd} Intern'l Cosmic Ray Conf., Calgary.
- Donn MacMinn and Joel Primack, "The Infrared Extragalactic Background and a New Cosmological Test" (senior thesis, U. of Calif. at Santa Cruz, 1994.) e-mail: pericles@scipp.ucsc.edu. Also submitted to Nature.
- S. Ogio *et al* (1993), in Proc. 23^{rd} Intern'l Cosmic Ray Conf., Calgary.
- E. Paré *et al* (1994), "Gamma-ray Astronomy: Extension Beyond the GeV Domain by Ground-based Observations", submitted to Physics Letters.
- M. Punch *et al* (1992) Nature **358**, 477.
- P.T. Reynolds *et al*, Ap. J. **404** (1993) 206.
- M.T. Ressel & M.S. Turner (1989),"The Grand Unified Photon Spectrum", in Comments on Astrophysics. Also Fermilab-pub-89/214-A.
- M.H. Salamon, F.W. Stecker, O.C. DeJager, "A New Method for Determining the Hubble Constant from sub-TeV Gamma-ray Observations", Ap. J. Lett., March 1, 1994, and references therein. (I have drawn heavily from their papers in the absorption discussion.)

- M. Stiavelli, 1994, these proceedings. There is also a nice review of "Unified Models of AGN's" in the Ann. Rev. of Astro. and Astrophysics for 1993.
- T. Tumar *et al* (1991), "Proposal for an Gamma Ray Telescope at Solar-1". (University of California at Riverside).
- M. Urban *et al*, Nucl. Phys. **14B** (1990) 223 (proc. supplement).
- G. Vacanti *et al* (1991), Ap. J. **377**, 401.
- Trevor Weekes, "Very High Energy Gamma-Ray Astronomy", Physics Reports **160** (1988) 1.

October 5, 1994

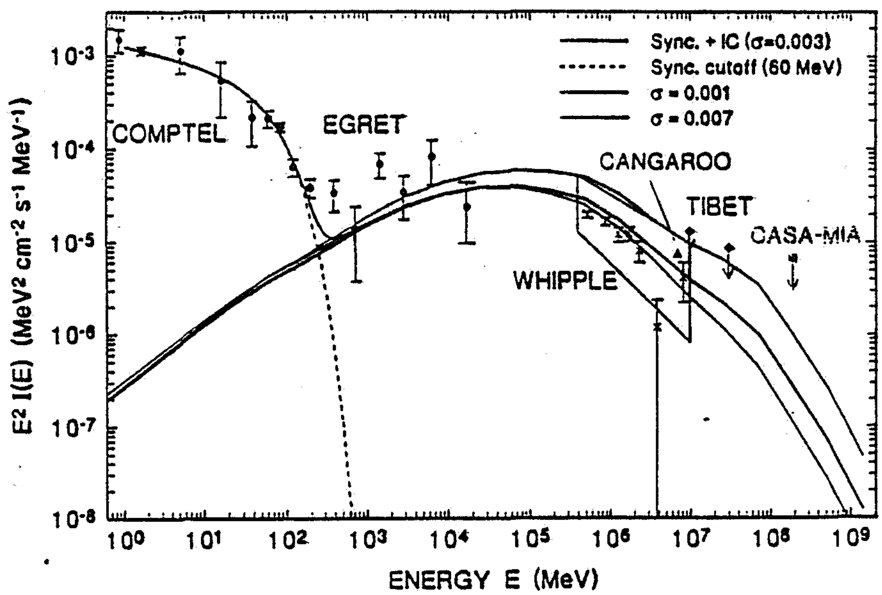

Figure 13: Gamma ray spectrum from the Crab nebula, measured by CGRO (Comptel and Egret) and by several ground-based experiments(Harding 1994).